JOURNAL OF Materials CHEMISTRY
Feature Article

Synthesis of sol–gel encapsulated heme proteins with chemical sensing properties†

Esther H. Lan,[a] Bakul C. Dave,[b] Jon M. Fukuto,[a] Bruce Dunn,*[a] Jeffrey I. Zink[c] and Joan S. Valentine[c]

[a]*University of California, Los Angeles, Department of Materials Science and Engineering, Los Angeles, CA 90095, USA*
[b]*Southern Illinois University, Department of Chemistry, Carbondale, IL, USA*
[c]*University of California, Los Angeles, Department of Chemistry and Biochemistry, Los Angeles, CA 90095, USA*

Received 18th May 1998, Accepted 16th July 1998

Heme proteins such as cytochrome-c (cyt-c), hemoglobin (Hb), and myoglobin (Mb) have been successfully encapsulated in sol–gel derived silica matrices, retaining their spectroscopic properties and chemical function. The thermal stability of cyt-c was significantly improved by immobilization in a porous silica network. Results from optical absorption, resonance Raman, and thermal denaturation studies suggest that biomolecules such as cyt-c design self-specific pores in the silica network according to the size and shape requirements of the biomolecule. Hb and Mb, immobilized using the sol–gel process, bound ligands similar to the proteins in aqueous buffer, and silica-encapsulated manganese myoglobin (MnMb) was a viable detector for nitric oxide (NO).

Introduction

The encapsulation of proteins in sol–gel derived silica glasses has been widely studied in recent years. Research in this field has established that, upon encapsulation, proteins retain their spectroscopic properties and enzymes retain their biological activity.[1–4] Immobilizing proteins by physically trapping the molecules in individual pores of a matrix permits the protein molecules to be isolated and stabilized. Conventional immobilization techniques such as covalent attachment results in chemical modifications of the protein. In contrast, sol–gel immobilization is characterized by physical entrapment without chemical modification. One potential advantage is that the silica matrix 'cages' the biomolecule, providing a far more 'rugged' environment for the dopant molecule in contrast to surface attachment schemes. The reaction chemistry of sol–gel immobilized biomolecular systems has been shown to be analogous to that in aqueous solution except for the observed rates of chemical reactions which are generally slower due to diffusion limitations in a porous silica matrix. The first studies on sol–gel immobilization of biomolecules by Avnir and coworkers involved trapping of the enzyme alkaline phosphatase which produced a bioactive powder.[5] We developed synthesis conditions that produced optically transparent monoliths with trapped proteins, enabling these materials to be used as optical sensors.[1]

Physical entrapment of proteins in a silica matrix without chemical modification preserves protein structure and functionality and protects the protein. Isolating protein molecules in individual pores of a silica matrix permits the molecules to be stabilized and prevents degradation due to proteases or microorganisms. In general, sol–gel matrices are thermally and chemically stable, can be obtained in a variety of forms such as bulk monoliths or thin films, and can store very high concentrations of proteins due to the porous network. Proteins and enzymes encapsulated in sol–gel derived glasses can interact with target molecules with a high degree of specificity, and using an appropriate sensing scheme, produce a detectable signal. While the relatively large biomolecules are immobilized within the silica network, the porous network allows small ions or molecules to be transported into the interior of the matrix. There is, however, a limit in the molecular size of the analyte that can be detected since it must be able to travel through the pore network.

At the time of gelation, the matrix may be considered as a two-phase system consisting of a porous solid and a trapped aqueous phase. This two-phase material is termed an aged gel. As the gel is allowed to dry, liquid is expelled from the pores and the gel shrinks as the pores collapse, forming a dried gel, termed a xerogel. Xerogels are approximately one-eighth of the original volume, 50% porous (by volume), and dimensionally invariant. The pores of the gels are negatively charged (pI of silica *ca.* 2) at the pH of the buffers ($pH \approx 7$) generally used to encapsulate biomolecules in the sol–gel process. Such pores can show affinity towards polar and charged dopant molecules, and they may also alter peripheral hydrogen-bonding interaction of biomolecules. As the conformations of the biomolecules are maintained by a large sum of relatively weaker non-covalent interactions, these effects can perturb the structural dynamics of trapped entities. The entrapment of biomolecules inside this silicate 'cage', therefore, can produce slight alterations in conformational structure and possibly biological function.

In this paper, we will review the literature published to date on sol–gel encapsulation of heme proteins and summarize the key findings. Proteins containing heme are characterized by the presence of Fe-protoporphyrin IX, which gives the protein its characteristic spectroscopic properties. In addition to reviewing the literature in this area, we include new studies on the heme proteins cytochrome c (cyt-c), hemoglobin (Hb), myoglobin (Mb), and manganese myoglobin (MnMb). For cyt-c, we investigated possible modifications to protein structure as a result of encapsulation, the extent to which the matrix can stabilize the protein from thermal denaturation, and the effect of pH on the protein in silica as compared to the protein in solution. For Hb, Mb, and MnMb, we evaluated the feasibility of using sol–gel encapsulated heme proteins as sensing elements, specifically, for optical detection of nitric oxide (NO). We and other research groups have investigated the sol–gel encapsulation of heme proteins for several reasons: 1) they represent model systems for understanding sol–gel

†Basis of the presentation given at Materials Chemistry Discussion No. 1, 24–26 September 1998, ICMCB, University of Bordeaux, France.

encapsulation effects as their protein structure and functionality have been well documented in the literature, 2) their characteristic spectroscopic properties make optical detection possible, 3) they can bind ligands, resulting in changes in optical absorption that are readily observed, and 4) they serve as feasible detectors for the ligands of interest, making device applications possible.

Experimental

Silica sol was prepared using tetramethylorthosilicate (TMOS) as the precursor. 15.27 g of TMOS, 3.36 g of deionized water, and 0.22 g of 0.04 M HCl were mixed and sonicated to produce the sol. For cyt-c, the sol was added to a Fe(III) cyt-c solution buffered with 0.1 M pH 4.25 acetate to achieve a final protein concentration of 100 μM in the aged gels. For Hb, Mb, and MnMb, the pH of the sol was raised to pH ≈ 5.5 using 1.0 M NH_4OH and then added to an aqueous protein solution. The final protein concentrations in aged gels were 5 μM for native Hb, 20 μM for native Mb, and 3 μM for MnMb. All proteins were encapsulated with the heme in the Fe(III) or Mn(III) state. Gels were of dimensions *x* 1.8 cm × 1.0 cm × 0.4 cm.

In the CO binding experiments with native Hb or Mb silica gels, aged gels with the protein in the Fe(III) or 'met' state were immersed in buffer (0.1 M pH 7.0 Tris–HCl), reduced with dithionite, and then exposed to gaseous CO, all under anaerobic conditions. The gels were gently stirred in CO-saturated buffer for 20 min. The saturation concentration of CO in water (1 atm, 20 °C) is 1 mM.[6] In the NO binding experiments with native Hb or Mb silica gels, aged gels in the Fe(III) or 'met' state were immersed in buffer and exposed to gaseous NO under anaerobic conditions. NO binding to Hb or Mb did not require reduction using sodium dithionite as NO can act as the reducing agent. The gels were gently stirred in the NO-saturated buffer for about 20 min. The saturation concentration of NO in water (1 atm, 20 °C) is 2 mM.[6]

MnMb was prepared by incorporating Mn protoporphyrin into apomyoglobin using the method of Yonetani and Asakura.[7] The experiments carried out using MnMb included the study of reactions in solution as well as in a sol–gel matrix. All experiments were conducted in air. In the experiments involving NO-synthase to enzymatically generate NO, the following constituents were mixed in the stated order: 1) 25 μl 0.01 M pH 7.4 Tris–HCl buffer, 2) 25 μl 0.2 mg ml^{-1} calmodulin, 3) 25 μl 40 mM $CaCl_2$, 4) 25 μl 2 mM NADPH, 5) 50 μl 1 mM tetrahydrobiopterin, 6) 25 μl 5 mM L-arginine, 7) 30 μl 60 μM MnMb solution, 8) 20 μl 57.5 mM sodium dithionite, and 9) 350 μl 341 μg ml^{-1} NOS enzyme solution (semi-purified from rat brains). The temperature of this solution was maintained at 37 °C during the experiment. In MnMb solution experiments with various nitrogen oxides, MnMb in 0.1 M pH 7.0 phosphate buffer was reacted with sodium dithionite and exposed to gaseous NO, gaseous NO_2, solid $NaNO_2$, solid $Na_2N_2O_3$, or solid $NaNO_3$ of the stated concentrations. For the sol–gel encapsulated MnMb, aged gels were immersed in buffer, reduced using sodium dithionite, and exposed to a 0.8 mM NO solution. In the *S*-nitroso-*N*-acetylpenicillamine (SNAP) experiments, aged gels were placed in buffer, reduced with dithionite, and then SNAP was added to the solution. Gels were immersed in the SNAP solution for the stated times.

Optical absorption spectra were measured using a Shimadzu UV-260 or Cary 3E spectrophotometer. Resonance Raman spectroscopy was performed on cyt-c by exciting the samples at 514.5 nm (Q-band). Excitation at 406.7 and 413.1 nm laser lines (Soret band) were not feasible as the thermal energy led to cracking of the gel samples. The cyt-c used for resonance Raman studies was in the Fe(III) state and had concentrations of 50 mg ml^{-1} and 25 mg ml^{-1} for solution and sol–gel samples, respectively. Thermal profile measurements were performed on a spectrophotometer equipped with circulating water which had its temperature controlled by a thermal programmer. The absorbance at 400 nm was monitored at 5 °C intervals from 25 to 95 °C. Effects of pH were tested by immersing a gel in phosphate buffer adjusted to appropriate pH values between 7 and 0. The gel was equilibrated with the buffer for about one day. The same sample was used throughout the length of the experiment.

Review of sol–gel encapsulation of heme proteins

Table 1 summarizes the research to date on sol–gel encapsulation of heme proteins and the key findings. Our earliest work on sol–gel encapsulation of proteins and enzymes demonstrated that optical spectroscopy of encapsulated cyt-c and Mb was essentially identical to that in solution.[1] In subsequent work on cyt-c, we found that immobilizing the protein in a silica matrix can stabilize the protein from aggregation due to methanol, and denaturation due to methanol was reversible in the encapsulated protein.[8] The improvements in protein stability in the presence of alcohol were attributed to confinement and isolation of the biomolecule in pores of the silica network. In work by Shen *et al.*, native cyt-c and zinc cyt-c were encapsulated in sol–gel silica glasses and studied using optical spectroscopy, circular dichroism, and resonance Raman spectroscopy.[9] The results collectively suggested that encapsulation in the sol–gel glass only slightly perturbed the polypeptide backbone and did not detectably perturb the heme group. In zinc cyt-c quenching experiments using $[Fe(CN)_6]^{3-}$, O_2 and *p*-benzoquinone, rate constants were consistently lower in the silica-encapsulated samples than in solution. The slower rates can be attributed to diffusion processes through the porous network. Moreover, changes in ionic strength and pH affected kinetics differently in the gel as compared to solution, possibly due to the fact that positively charged cyt-c adsorbed to the negatively-charged silica walls.

The encapsulation of cyt-c–cyt-c peroxidase complexes in sol–gel derived gels allowed, for the first time, detection of this system's electron paramagnetic resonance (EPR) signals at room temperature.[10] Previously, quantitative EPR measurements of cyt-c and its complexes were performed at temperatures below −100 °C, because EPR absorption of the heme group broadens at higher temperatures. By sol–gel encapsulation, however, a suitable microenvironment was obtained that permitted a measurable EPR spectrum at ambient temperatures because the immobilized protein was 'frozen' in the gel. The charge transfer activities between the Fe and porphyrin ring in cyt-c–cyt-c peroxidase complex were weak in the silica gels as compared to that in solution. Redox processes of the encapsulated cyt-c–cyt-c peroxidase complex were more active in the aged gel stage than in the xerogel stage.

In one study to evaluate biocatalysis of sol–gel encapsulated heme proteins, the sol–gel encapsulated proteins (cyt-c, Mb, Hb, horseradish peroxidase) had catalytic efficiencies in the oxidation of dibenzothiophene similar to those in solution.[11] Because of the advantage of easy separation of the encapsulated proteins from the liquid reaction mixture, it was suggested that immobilization of active heme proteins in the solid glass media could serve as a more practical biocatalysis. In another study to evaluate the cooperativity of O_2 binding, the quaternary protein Hb was immobilized in both aerobic and anaerobic silica thin films.[12] In both cases, O_2 binding to the Hb was non-cooperative. This is in contrast to solution, where it has been well established that O_2 binding is cooperative. The conclusion drawn from these studies was that Hb encapsulated in the sol–gel glasses remained fixed in their original quaternary structures during the oxygenation or deoxygenation process. It is likely that structural changes were not totally forbidden but the kinetics were considerably slowed by sol–gel encapsulation. This finding is quite interesting as it implies that sol–gel encapsulation can preferentially dictate the quaternary

Table 1 Review of research on sol–gel encapsulation of heme proteins

Heme protein(s)	Purpose of study	Finding(s)	Ref.
cyt-c, Mb, Hb	Biological function: ligand (O_2, CO, NO) binding	Oxidation–reduction properties of heme and ligand binding similar to that in solution	1 (1992) 13 (1994)
cyt-c, Mb, Hb, horseradish peroxidase	Biocatalysis: oxidation of dibenzothiophene	Catalytic activities similar to that in solution	11 (1994)
Hb	Oxygen binding: evaluation of cooperativity	Oxygen binding to Hb in sol–gel systems non-cooperative. Quaternary structures of Hb 'fixed' upon encapsulation	12 (1994)
cyt-c, Mb, Hb	Ligand binding and sensing	Ligand binding similar to that in solution and higher absorption intensity with increasing ligand concentration	14 (1995)
Mb	Sensing of dissolved oxygen (DO) in water	DO concentrations at ppm levels can be measured within minutes	16 (1995)
Mb	Sensing of DO in water	Detection limit for DO can be enhanced using fluoresence instead of absorbance signals	17 (1996)
cyt-c and cyt-c peroxidase	Spin state and charge transfer activity	Charge transfer activities between cyt-c and cyt-c peroxidase weak in sol–gels compared to that in solution	10 (1996)
cyt-c	Kinetics of photo-induced electron transfer reactions	Encapsulation did not detectably perturb heme group but different reaction kinetics observed in sol-gel *vs.* solution	9 (1997)
cyt-c	Effect of alcohol (and other synthesis conditions) on protein stability	Encapsulation stabilized protein against aggregation due to methanol and made denaturation reversible	8 (1997)
cyt-c, Mb	Binding to CO_2	Formation of MetMb–CO_2 adduct possible in sol–gels whereas MetMb in solution denatures upon CO_2 exposure	15 (1998)

structure of proteins, opening new areas of protein structure–function relationships.

Since heme proteins such as Hb and Mb bind ligands O_2, CO, and NO, by encapsulating these proteins in silica matrices, it is possible to create solid-state materials which can be used as sensing elements for these gases. The findings have been consistent in that formation of O_2, CO, or NO adducts in sol–gel encapsulated Hb and Mb is similar to those adducts in solution, as observed using optical spectroscopy.[1,13,14] Ligand binding experiments with the native heme proteins were conducted anaerobically. The formation of these adducts was reversible. Table 2 details the spectroscopic characteristics of Hb and Mb in the unligated [met or Fe(III)] and ligated (CO, NO) forms. Aged silica gels with Hb or Mb in the Fe(III) state can be stored for at least one year with no significant changes in spectroscopy or ability to bind ligands.

From Table 2, it is apparent that upon CO binding, silica-encapsulated HbCO and MbCO exhibited the same spectroscopic features as in solution. Fig. 1 shows the absorption spectra of metHb/HbCO and metMb/MbCO in solution and in silica gels. Upon NO binding, silica-encapsulated MbNO also exhibited the same spectroscopic features as in solution, although the Soret band for HbNO was slightly blue shifted as compared to that in solution. The slight blue shift in the HbNO Soret band was consistently observed (Table 2).

Table 2 Optical absorption characteristics of heme proteins

State of protein	Soret/nm		β/nm		α/nm		Ref.
	Soln.	Sol–gel	Soln.	Sol–gel	Soln.	Sol–gel	
MetMb	409	409					13
	410	410					14
MbCO	423	423	541	541	578	578	13
	424	424	542	540	578	578	14
MbNO	418	418	533	533	574	574	13
	418	418	534	534	574	574	14
MetHb	406	406					13
	406	406					14
HbCO	420	420	538	538	569	568	13
	420	420	540	540	570	566	14
HbNO	418	416	535	533	567	565	13
	416	412	534	530	566	562	14

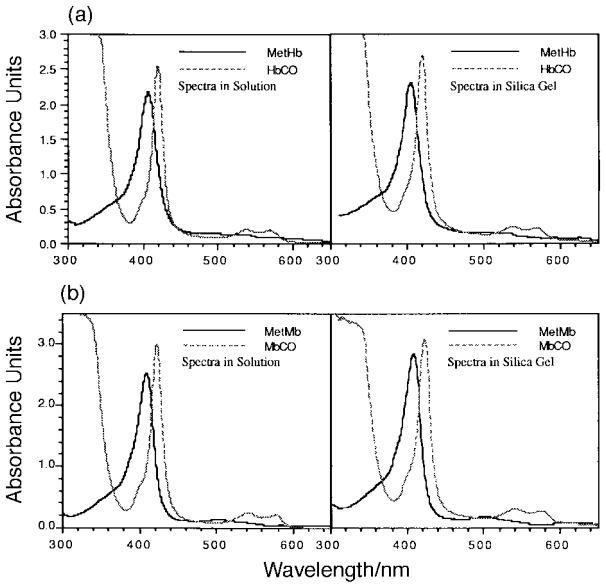

Fig. 1 (a) Optical spectra of MetHb and HbCO indicate successful CO binding in the silica-encapsulated Hb, resulting in the same spectroscopic changes as those observed in aqueous buffer. (b) Optical spectra of MetMb and MbCO in aqueous buffer and aged silica gel also show the same spectroscopic changes upon CO binding.

Fig. 2 shows the absorption spectra of MetHb/HbNO and MetMb/MbNO in solution and in silica gels. In a recent study, the encapsulation of MetMb in sol–gel derived gels permitted formation of a CO_2 adduct.[15] This contrasts dramatically with the behavior of MetMb in solution, where it denatures when exposed to CO_2. Therefore, sol–gel encapsulation made possible a CO_2 complex which could not be obtained in aqueous buffer.

Since the heme proteins retain their reactivity in optically transparent glasses, these materials can be used as sensing elements. We have used sol–gel encapsulated Mb as a sensing element for measurement of dissolved oxygen in water using optical spectroscopy.[16] The dissolved oxygen concentration was determined quantitatively by observing the rate of change of the visible absorption spectrum. The overall change in

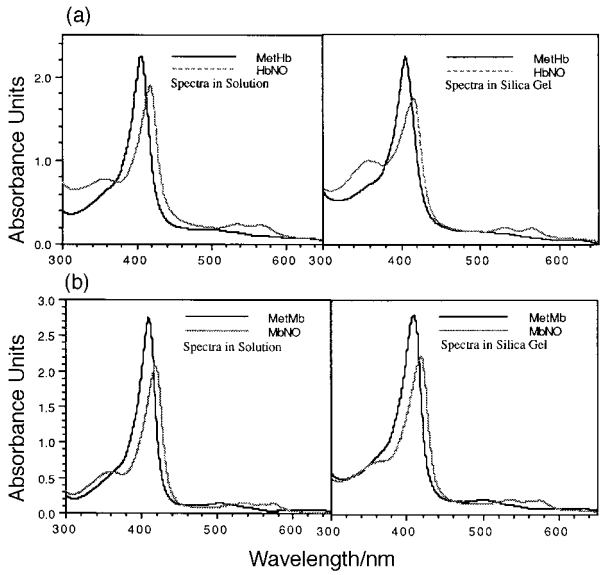

Fig. 2 (a) Optical spectra of MetHb and HbNO indicate successful NO binding in the silica-encapsulated Hb. The spectroscopic changes are the same as those in aqueous buffer, except for a slight blue shift in the Soret peak maximum and decrease in intensity. (b) Optical spectra of MetMb and MbNO in aqueous buffer and aged silica gel also show the same spectroscopic changes upon NO binding.

absorbance at 431.5 and 436 nm was linear with time and directly proportional to the concentration of dissolved oxygen. The dissolved oxygen concentrations examined in the study ranged from 2 to 8 ppm. Moreover, the optical response can be established rapidly as the rate of absorbance change was established within 2 min. The gels were also reusable since O_2 binding is reversible, and used gels can be regenerated to metMb by 'washing' with aerated buffer to remove the dithionite. Mb encapsulated in sol–gel silica proved to be an accurate and reproducible sensing element for measurement of dissolved oxygen at ppm concentrations. In a subsequent study, the fluorescent dye brilliant sulfaflavine was used to enhance the detection limit for DO measurements.[17]

The accumulation of research data on heme proteins clearly demonstrate that these proteins retain their characteristic optical signatures and chemical function upon sol–gel encapsulation. By isolating and 'caging' the biomolecules in a porous silica matrix, interesting effects and new features have been observed, such as 1) cyt-c was stabilized from aggregation in methanol and methanol denaturation was reversible, 2) electron paramagnetic resonance on cyt-c could be performed at room temperature, 3) a MetMb–CO_2 adduct was formed which was not possible in aqueous buffer, and 4) the quaternary structure of a polymeric protein such as Hb could be 'fixed'. In addition, sol–gel immobilized heme proteins can bind ligands such as O_2, CO, and NO. Results with O_2 and immobilized Mb demonstrated that O_2 concentrations can be quantitatively determined in a matter of minutes. Therefore, these protein-doped glasses can be explored as potential solid-state optical detectors and sensors.

Encapsulation of cytochrome c: biomolecules that design self-specific pores

Cytochrome c is an electron transport protein in which its heme Fe is reversibly oxidized and reduced between the Fe(II) and Fe(III) oxidation states.[18,19] Its absorption signature has been carefully studied and established in solution. We report here our investigation of cyt-c to determine changes in its structure as a consequence of sol–gel encapsulation and gel drying. A biomolecule such as cyt-c, by virtue of a relatively high molecular weight ($\approx$12,400 Da) and high positive charge, is likely to interact with the silica pore walls. In this section, we specifically address the following issues: 1) the influence of the silica matrix on the protein upon encapsulation and subsequent gel drying, 2) thermal denaturation of silica-encapsulated cyt-c, and 3) pH effects on silica-encapsulated cyt-c.

Optical absorption and resonance Raman studies

Absorption spectra of Fe(III) cyt-c in solution (0.1 M acetate, pH 4.5) and encapsulated in an aged silica gel (equilibrated with 0.1 M acetate, pH 4.5) are shown in Fig. 3. In the aged state, the pores are filled with liquid and there has been no change in the original volume of the gel. Both samples exhibited the characteristic pattern of cyt-c, indicating that the heme signature is preserved upon encapsulation of the protein in the gel. Although the overall characteristics are similar, slight changes in peak wavelengths are observed. The spectrum of the protein in solution shows the Soret band maximum at 406 nm, while the spectrum of the protein in an aged gel shows a slight blue shift in the Soret band maximum from 406 to 404 nm. The slight blue shift of cyt-c upon encapsulation was also observed by Blyth *et al.* wherein the solution had its Soret band maximum at 410 nm, while the sol–gel sample had its Soret band maximum at 408 nm.[14] In their experiments, the samples were equilibrated with pH 7.0 phosphate buffer.

Xerogels were prepared by ambient drying of the aged gel samples. During the transformation to the xerogel state, there are both weight and volume changes. In the xerogel state, most of the liquid in the pores has evaporated, accompanied by a collapse of the pores and a considerable shrinkage in volume. The xerogel is typically $\approx$15% of the original volume and $\approx$20% of the original weight. The spectrum of cyt-c in a xerogel is shown in Fig. 4. As previously reported,[8] the blue shift in the cyt-c Soret band continues along the aged gel to xerogel transition in the silica matrix, with the xerogel sample showing a Soret band maximum at 395 nm. There is a total downshift of 9 nm (from 404 to 395 nm) that can be attributed to drying effects. These effects arise due to either pore collapse or to loss of solvent phase from the aged gel samples that occurs during drying.

In order to determine the exact cause of the blue shifts, absorption spectra were obtained on rehydrated xerogel samples. Xerogels were rehydrated with 0.1 M acetate buffer (pH 4.5), with no swelling of the gels. Absorption spectra of xerogels immersed in solution show a distinctly red shifted

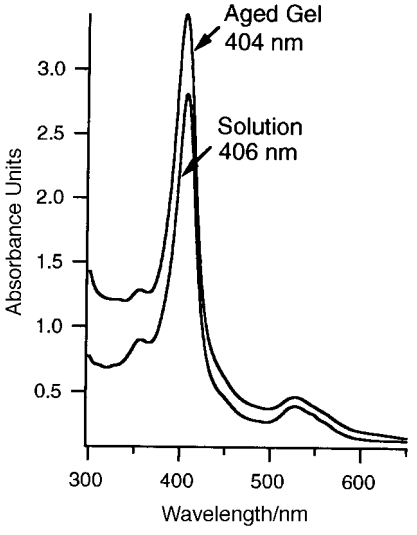

Fig. 3 Optical spectra of cyt-c in aqueous buffer and aged gel show a slight blue shift in the Soret band maximum for the aged gel (404 nm) as compared to aqueous buffer (406 nm).

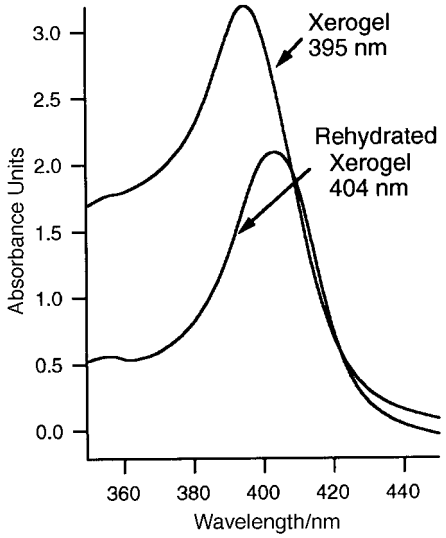

Fig. 4 Upon drying, the xerogel cyt-c Soret band is further blue shifted to 395 nm. After rehydration, however, the Soret band is red shifted back to 404 nm, the same value as that for an aged gel. The blue shift in the Soret band that accompanies drying, therefore, is reversible upon rehydration.

Soret band that once again has its maximum at 404 nm, as shown in Fig. 4.[8] This value is exactly the same as that observed for aged gel samples. Thus, there is a *reversible* 9 nm shift in the Soret band maximum that accompanies drying and subsequent rehydration. The reversibility of these shifts indicates that the blue shift during drying was due to evaporation of the solvent phase and not due to physical constraint of the protein from pore collapse. The reversibility of the Soret band shift upon rehydration in xerogels suggests that cyt-c experienced similar metal–heme interactions in the xerogels as in aged gels even after substantial shrinkage in gel volume and pore size.

Resonance Raman (RR) frequencies for Fe(III) cyt-c in solution, aged gel, and rehydrated xerogel are summarized in Table 3, along with mode assignments.[20] It was not possible to obtain spectra on dried xerogel samples due to thermally induced sample cracking under laser irradiation. For the rehydrated xerogel samples, only the strongly enhanced modes could be observed due to extensive background and poor signal to noise ratio. As seen in Table 3, the overall spectral pattern is preserved upon sol–gel encapsulation, although a few peaks were upshifted. The RR frequencies for the aged and rehydrated xerogel samples were essentially the same, indicating that the structure of the heme group in xerogels was not substantially altered as compared to that in aged gels. Results from RR suggest that volume shrinkage during gel drying did not significantly alter the ground state geometry of the heme in cyt-c. RR studies on cyt-c by Shen and Kostic showed all vibrational bands in the solution and sol–gel samples had identical wavenumbers within experimental error.[9] The relative intensity of most bands also remained unchanged,

Table 3 Resonance Raman frequencies (cm^{-1}) of cytochrome-c

Mode assignment[20]	Cyt-c in aqueous buffer	Cyt-c in aged gel	Cyt-c in rehydrated xerogel
ν22	1130	1131	
ν30	1175	1175	1172
ν13	1232	1235	
ν21	1315	1317	1318
ν4	1366	1370, 1376	1376
ν29	1404	1410	1410
ν11	1551	1553	
ν19	1584	1590	

leading to the conclusion that the sol–gel encapsulation did not appreciably alter the spin state, oxidation state, or geometry of the heme site.

The finding that both the aged and rehydrated xerogels had the same optical absorption and RR characteristics suggests that the microenvironment of cyt-c is not influenced by the stresses caused by pore shrinkage during drying. One mechanism which could account for this behavior is that the biomolecule designs a self-specific pore as the silica network forms from hydrolysis and condensation reactions during the sol–gel process. That is, the silica cage that defines the pore forms around the biomolecule according to the size and shape requirements of the biomolecule. The presence of the biomolecule prevents its surrounding pore from collapsing during gel drying.

Thermal denaturation studies

Globular proteins such as cyt-c possess non-covalent interactions (hydrogen bonds, van der Waals bonds, *etc.*) that maintain the native folded state under physiological conditions. Disruption of the non-covalent interactions by thermal energy leads to denaturation by unfolding. Thermally induced unfolding of the proteins in solution, in general, is highly cooperative with a sharp transition over a small temperature range. The transition point at which half of the molecules are denatured is termed T_m. The increased intensity of the cyt-c heme Soret band in the unfolded state as compared to the native state can be used to monitor the thermal denaturation process,[21,22] and optical monitoring of the heme band at 400 nm was used in the experiments described here. As shown in Fig. 5, the solution sample of cyt-c (0.1 M sodium acetate buffer, pH 4.5) showed a transition to the denatured state with a $T_m \approx 65\,^{\circ}C$, whereas the aged gel sample (equilibrated with 0.1 M sodium acetate buffer, pH 4.5) did not show any transition up to *ca.* 95 °C. For the sol–gel sample, it was not possible to increase the temperature beyond 95 °C as boiling of the buffer led to gel cracking. Since both experiments were performed under the same conditions, the observed increase in thermal tolerance of the protein can be ascribed to the influence of the silica gel matrix.

The thermal denaturation experiments underscore the pronounced influence of the physical effects of caging. The

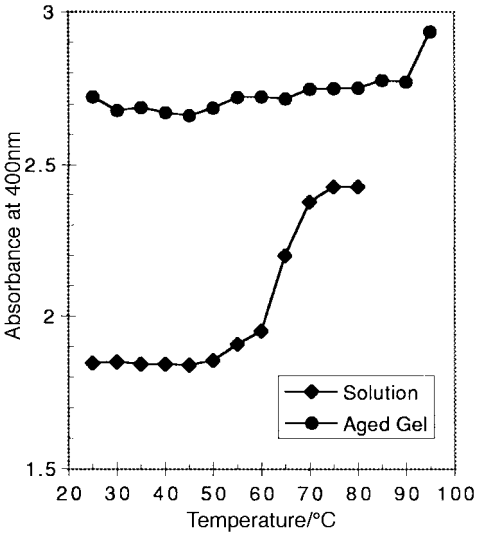

Fig. 5 Thermal denaturation profiles of cyt-c in aqueous buffer and in an aged gel indicate that there is a substantial improvement in thermal stability as a result of sol–gel encapsulation. $T_m \approx 65\,^{\circ}C$ in aqueous buffer, whereas denaturation does not begin until *ca.* 95 °C in the aged gel. It was not possible to increase the temperature beyond 95 °C as boiling of the buffer led to gel cracking. The absorbance values are higher for the aged samples than for the solution sample because of a higher cyt-c concentration in the aged gel.

substantial stability provided by the matrix supports the hypothesis that the protein molecules dictate the required size of its surrounding pore. The presence of a rigid cage structure around the protein then restrains the conformational mobilities of the protein thereby thermally stabilizing it against thermal denaturation.

pH Studies

Conformations of cyt-c are pH dependent and several conformational transitions accompany changes in pH.[23,24] In the acidic region, at least two pH induced transitions have been characterized, one centered at pH $\approx$ 3 and the other at pH $\approx$ 1. It has been concluded that the transitions accompany a change in the spin-state of the central Fe atom. There is a high-spin configuration of the Fe(III) at low pH as compared to a low-spin configuration existing at neutral pH. The transition centered around pH $\approx$ 3 has been characterized as due to replacement of axial Met-80 residue with Lys-79, whereas the transition centered around pH $\approx$ 1 probably involves replacement of both axial residues with terminal water molecules.[25]

Optical monitoring of the Soret band wavelength at different pH values provides a good estimate of the pH induced conformational changes in the protein. Overall conformational changes occur in the protein as the polypeptide subunits are protonated or deprotonated. At pH > 4, the solution spectrum shows its Soret band maximum centered at 406 nm which shifts to *ca.* 395 nm at pH 1. The optical absorption changes indicate a titration of the amino acid groups with the protons. In solution, two transitions centered around pH $\approx$ 0 and pH $\approx$ 3 can be observed, as shown in Fig. 6. Within the limits of experimental error, these values correspond well with the reported literature. On the other hand, similar experiments on cyt-c encapsulated in aged gels indicate a more continuous variation in the pH profile, also shown in Fig. 6. A large change in Soret peak wavelength is observed in the pH range 3 to 5 with a midpoint at pH $\approx$ 4. At low pH, the sharp transition observed in solution is no longer evident in the aged gel samples. Instead the conformational change accompanying pH variation is spread out over a pH range of 3 to 0.

The observed differences in the proton dependent behavior of the cyt-c in solution and in aged gels show that the presence of the silica matrix may have altered the acid–base properties of the protein. As changes in pH induce conformational transitions in cyt-c, it is possible that the constraints imposed by encapsulation within a pore of finite dimension restrict those transitions. Another possibility is that the charged residues on cyt-c react differently with the pore walls of the silica matrix depending upon pH. Whether the difference is due to the matrix hindering conformational transitions or due to the charged silicate groups on the matrix surface (pI $\approx$ 2) interacting with the charged residues on cyt-c cannot be resolved with the current data.

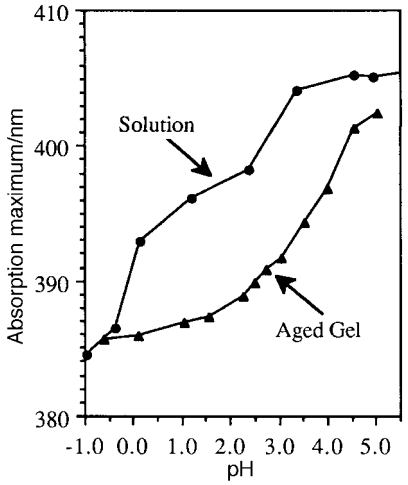

Fig. 6 Optical monitoring of the Soret band wavelength as a function of pH shows a difference in the proton-dependent behavior of cyt-c in aged silica gels as compared to aqueous buffer.

In summary, our studies on cyt-c revealed that the overall structure of this protein is retained upon sol–gel immobilization, although there may be subtle differences with respect to protein conformation. Optical absorption spectra showed a blue shift in the spectrum as a result of encapsulation in aged gels that became more pronounced in xerogels. Upon rehydration of the xerogel, however, the effects were *reversible* to the aged gel state. The results suggest that the protein dopant forms a self-specific 'cage', so that even as pores collapse, there is minimal change in the physical constraint imposed by the matrix. Our thermal studies demonstrated one of the benefits of sol–gel encapsulation, that thermal stability of the protein was significantly improved in immobilized cyt-c. While cyt-c in solution undergoes unfolding with a $T_m \approx 65\,^{\circ}C$, the protein encapsulated in the aged gel did not show any transition up to *ca.* 95 °C. The presence of the physical cage in the sol–gel matrix stabilizes the folded state as compared to the unfolded state. A similar improvement in protein stability to alcohol has also been observed for cyt-c in silica gels.[8]

Sol–gel encapsulated manganese myoglobin: detector for nitric oxide

As discussed previously, native Mb and Hb with Fe in the heme can bind O_2, CO, and NO. Manganese myoglobin (MnMb), however, is an excellent alternative to native Mb for NO detection because the manganese-substituted proteins bind NO but not O_2.[26] Moreover, NO-binding in MnMb can also be detected optically by using the α peak of MnMbNO at 580 nm as the optical marker.

Nitric oxide chemistry has been in the forefront of research recently because of its importance in physiological activities ranging from maintaining vascular tone to antimicrobial defense.[27] NO is synthesized in cells *via* the oxidation of L-arginine to L-citrulline by the enzyme NO synthase (NOS), as shown in eqn. (1).

$$\text{L-arginine} \xrightarrow{O_2,\ \text{NADPH, NOSynthase}} \text{L-citrulline} + \text{NO} \qquad (1)$$

NO is a free radical and the biological lifetime of NO is of the order of seconds. A variety of sensors have been developed to measure NO levels. A porphyrinic-based microsensor has been developed to detect NO electrochemically,[28] and optical methods have also been developed based on bacteria denitrification,[29] conversion of HbO_2 to metHb,[30] chemiluminescence of ozone treated NO,[31] luminol chemiluminescence,[32] guanylate cyclase activation,[33] and other NO-mediated effects.

More recently Aylott *et al.*[34] demonstrated that cyt-c can also be used for optical NO sensing. By using sol–gel thin films with encapsulated cyt-c, a reversible NO sensor was developed that can measure NO at ppm levels within minutes. Barker *et al.* developed a reversible fiber-optic NO sensor based on cyt-c′ that can also measure NO at ppm levels with <1 s response time. In both cases, there was no interference from O_{21} and with cyt-c′, interference from NO_2 can also be eliminated.

An ideal optical sensor for NO is one which specifically binds NO with high affinity, producing a measurable change in the absorption spectrum. The ability to conduct the experiments aerobically is also an important factor, since working in an O_2-free environment is physiologically unreasonable.

To evaluate the sensitivity of MnMb for NO sensing under simulated physiological conditions, we conducted an experiment in which NO was generated enzymatically from the

enzyme nitric oxide synthase (NOS). In this experiment, MnMb was in solution rather than in a silica gel so that NO transport would not be impeded by the silica matrix. The experiment was conducted in the presence of air. After mixing an aqueous solution of the NOS enzyme, L-arginine, the required cofactors and MnMb, optical absorption was recorded periodically between 500 and 600 nm to detect generation of NO as evidenced by the α peak of MnMbNO at 580 nm.

Fig. 7 shows the optical absorption of the NOS–MnMb solution as a function of time. The data clearly demonstrate that enzymatically generated NO can be detected optically by directly monitoring the NO adduct. The level of NO generated in the NOS–MnMb experiment was estimated by measuring the enzymatic activity, *i.e.* nmole of citrulline generated per mg of enzyme. As shown in eqn. (1), citrulline and NO are formed in equimolar amounts. The measured levels of citrulline generated per mg of NOS after 30, 60, 90, and 120 min were 161, 239, 212, and 256 nmol, respectively. In the experiment reported here *ca.* 0.12 mg of enzyme was used. Although optical detection of NO was reported previously using HbO_2,[30] MnMb represents a better choice of protein because one can measure the NO-adduct directly and also because HbO_2 will eventually oxidize to metHb without NO in the presence of air.

To determine the specificity of MnMb for NO sensing, we carried out control experiments in which MnMb in solution was reacted with other nitrogen oxides, specifically NO^-, NO_2, NO_2^-, and NO_3^-. All experiments were performed with MnMb in aqueous buffer. We found that MnMb binds NO^- and NO_2 but not NO_2^- or NO_3^-. NO^- was generated indirectly *via* the decomposition of $Na_2N_2O_3$, which releases HNO (NO^-) in aqueous solution[36] as shown in eqn. (2);

$$Na_2N_2O_3 = HNO + NO_2^- \quad (2)$$

NO_2^- does not bind MnMb. However, it produces NO at sufficiently high concentrations according to eqn. (3).

$$3HNO_2 = HNO_3 + 2NO + H_2O \quad (3)$$

Table 4 lists the different nitrogen oxide species tested and their ability or inability to bind MnMb.

We successfully encapsulated MnMb in optically transparent sol–gel derived silica gels and used these protein-doped materials as NO detectors. As mentioned previously, a significant advantage of using MnMb to detect NO is that experiments can be performed aerobically. Fig. 8 shows the absorption spectra of Mn(III)Mb, Mn(II)Mb, and MnMbNO in solution and in an aged silica gel. Optical absorption characteristics of MnMb and its NO adduct are detailed in Table 5. A comparison of the spectra shows essentially the same spectroscopic properties upon metal reduction and NO binding in the aged gel as in solution.

In addition to binding dissolved gaseous NO, silica-encapsulated MnMb can also bind NO released from a chemical. *S*-Nitroso-*N*-acetylpenicillamine (SNAP) releases NO in an aqueous medium.[37] Fig. 9 shows the absorption spectra of MnMb aged gels reacted with SNAP, and NO binding is evident. There was a predictable concentration effect as the 1.5 mM SNAP concentration required a longer incubation

Table 4 Reaction of nitrogen oxides with manganese myoglobin

Nitrogen oxide	Experimental conditions	NO-Binding
NO (gas)	[NO] = 0.8 mM	Yes
NO_2 (gas)	$[NO_2]$ = 3.7 mM	Yes
NO_2^- (solid $NaNO_2$)	$[NO_2^-] < 10$ mM	No
	$[NO_2^-]$ = 45 mM	Yes
NO^- (solid $Na_2N_2O_3$)	$[NO^-]$ = 5.5 mM	Yes
NO_3^- (solid $NaNO_3$)	$[NO_3^-]$ = 45 mM	No

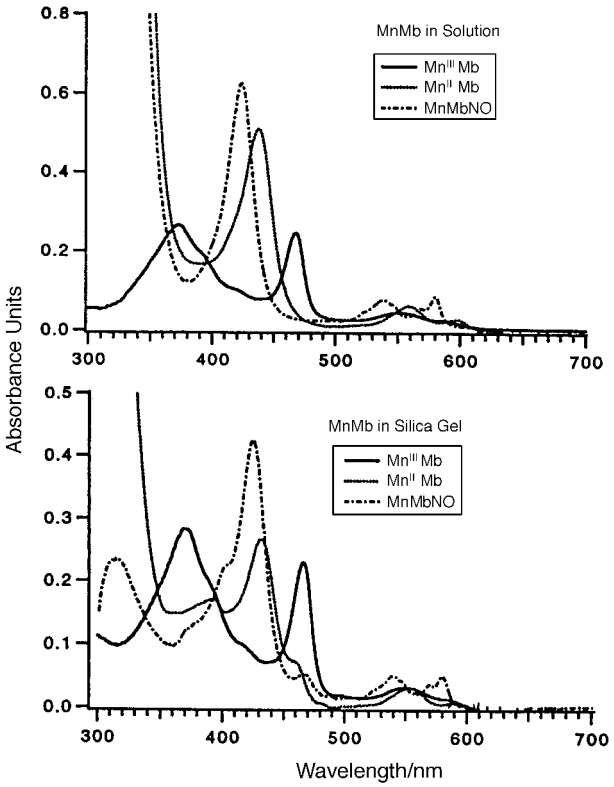

Fig. 8 Successful NO detection was achieved in silica-encapsulated MnMb, as the same characteristic absorption changes were observed upon metal reduction and NO binding as compared to MnMb in aqueous buffer. The slight reduction in absorption intensity for the aged gel was most likely caused by the decomposition of the reducing agent (sodium dithionite). The gel was immersed in a dithionite solution which became cloudy over time in air.

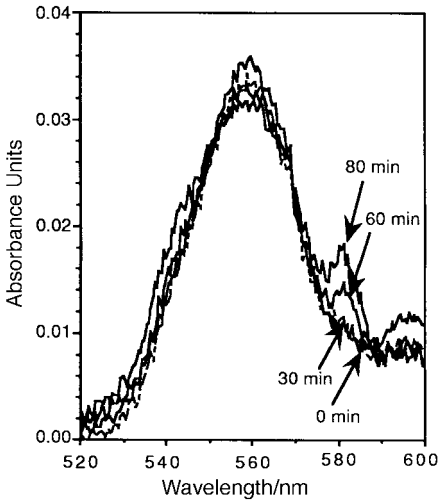

Fig. 7 Optical monitoring of a solution containing NO synthase and MnMb at varying incubation times demonstrates that NO generated by NO synthase can be detected. The α peak at 580 nm of MnMbNO was used as the optical marker for NO binding.

Table 5 Optical absorption characteristics of manganese myoglobin

	Soret/nm		β/nm		α/nm	
Description	Soln.	Sol–gel	Soln.	Sol–gel	Soln.	Sol–gel
Mn(III)Mb	373	371				
	468	468				
Mn(II)Mb	438	438				
Mn(II)MbNO	424	424	538	538	580	579

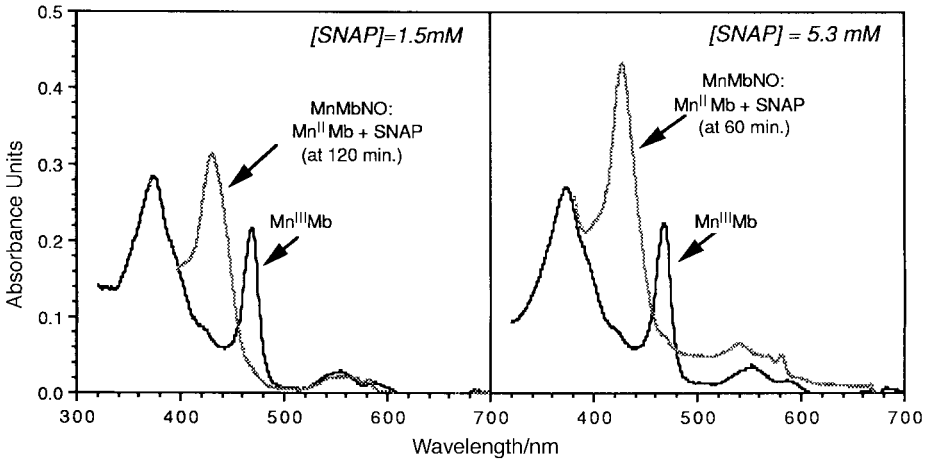

Fig. 9 Optical monitoring of MnMb in silica gels reacted with NO released from *S*-nitroso-*N*-acetylpenicillamine (SNAP) shows NO binding. As expected, there was a higher level of the NO adduct with a higher SNAP concentration.

time (> 120 min) for complete NO binding compared with the 5.3 mM SNAP concentration (⩽60 min).

These experiments demonstrate the potential for using encapsulated heme proteins in sol–gel matrices as sensing elements. A simple yet effective optically-based technique to detect NO was developed using sol–gel encapsulated MnMb. The Mn-substituted heme makes aerobic experiments possible, which is critical for physiological conditions. The advantages of using heme proteins [cyt-c, cyt-c′, MnMb] include direct detection of NO *via* formation of an NO-adduct and the ability to detect NO without interference from O_2 or air. One disadvantage of MnMb is that it is not specific for the NO free radical but will also react with NO^- and NO_2 to form MnMbNO. In sensor applications, the sol–gel encapsulated MnMb should be in thin-film form to maximize kinetics of analyte diffusion through the pores.

Conclusions

Heme proteins can be successfully encapsulated in silica matrices with minimal changes to their spectroscopic properties. Research by various groups has shown that the immobilized heme proteins also retain their chemical functions of oxidation/reduction, ligand (O_2, CO, NO) binding, and biocatalysis. The sol–gel encapsulated proteins can be used to quantitatively determine concentration of dissolved gases as dissolved O_2 concentrations could be measured within minutes. Moreover, immobilization using the sol–gel approach has enabled new features such as room temperature electron paramagnetic resonance, formation of a MetMb–CO_2 adduct, and fixation of Hb's quaternary structure. The conclusions from our new studies include the finding that encapsulation in a porous silica matrix can significantly improve the thermal stability of a protein.

Thermal denaturation studies on cyt-c demonstrated that whereas the protein in aqueous buffer showed a transition to the denatured state with $T_m \approx 65\,^{\circ}C$, the sol–gel immobilized protein did not show any transition up to *ca.* 95 °C. A similar improvement in protein stability to alcohol has also been achieved using sol–gel encapsulation. Another key finding from our studies was that sol–gel encapsulated MnMb can serve as solid-state detectors or sensors for NO. Our experiments established that sol–gel immobilized MnMb binds NO without interference from O_2, similar to MnMb in solution. Finally, an intriguing hypothesis based on collective results from optical absorption, resonance Raman, and thermal denaturation studies on cyt-c is that this protein designs self-specific pores in the silica network according to its size and shape requirements.

The authors thank Dr Yumiko Komori for preparation of the NOS enzyme and SNAP, Naiyma Houston and James Hauser for their experimental assistance, and Dr. Daryl Eggers for his critical reading of the manuscript. The support of this research by the National Science Foundation (DMR-9408780) is greatly appreciated.

References

1 L. M. Ellerby, C. R. Nishida, F. Nishida, S. A. Yamanaka, B. Dunn, J. S. Valentine and J. I. Zink, *Science*, 1992, **255**, 1113.
2 D. Avnir, S. Braun and M. Ottolenghi, in *Supramolecular Architecture in Two and Three Dimensions*, ed. T. Bein, American Chemical Society, New York, 1992.
3 B. C. Dave, B. Dunn, J. S. Valentine and J. I. Zink, *Anal. Chem.*, 1994, **66**, 1120A.
4 D. Avnir, S. Braun, O. Lev and M. Ottolenghi, *Chem. Mater.*, 1994, **6**, 1605.
5 S. Braun, S. Rappoport, R. Zusman, D. Avnir and M. Ottolenghi, *Mater. Lett.*, 1990, **10**, 1.
6 E. Antonini and M. Brunori, *Hemoglobin and Myoglobin in their Reactions with Ligands*, North-Holland Publishing, Amsterdam, 1971.
7 T. Yonetani and T. Asakura, *J. Biol. Chem.*, 1969, **244**, 4580.
8 B. C. Dave, J. M. Miller, B. Dunn, J. S. Valentine and J. I. Zink, *J. Sol–Gel Sci. Technol.*, 1997, **8**, 629.
9 C. Shen and N. M. Kostic, *J. Am. Chem. Soc.*, 1997, **119**, 1304.
10 C. T. Lin, C. M. Catuara, J. E. Erman, K. C. Chen, S. F. Huang, W. J. Wang and H. H. Wei, *J. Sol–Gel Sci. Technol.*, 1996, **7**, 19.
11 S. Wu, J. Lin and S. I. Chan, *Appl. Biochem. Biotechnol.*, 1994, **47**, 11.
12 N. Shibayama and S. Saigo, *J. Mol. Biol.*, 1995, **251**, 203.
13 E. H. Lan, M. S. Davidson, L. M. Ellerby, B. Dunn, J. S. Valentine and J. I. Zink, *Mater. Res. Soc. Symp. Proc.*, 1994, **330**, 289.
14 D. J. Blyth, J. W. Aylott, D. J. Richardson and D. A. Russell, *Analyst*, 1995, **120**, 2725.
15 Q. Ji, C. R. Lloyd, W. R. Ellis and E. M. Eyring, *J. Am. Chem. Soc.*, 1998, **120**, 221.
16 K. E. Chung, E. H. Lan, M. S. Davidson, B. Dunn, J. S. Valentine and J. I. Zink, *Anal. Chem.*, 1995, **67**, 1505.
17 M. F. McCurley, G. J. Bayer and S. A. Glazier, *Sens. Actuators B*, 1996, **36**, 491.
18 R. A. Scott and A. G. Mauk (Editors), *Cytochrome c: A Multidisciplinary Approach*, University Science Books, Sausalito, CA, 1996.
19 G. R. Moore and G. W. Pettigrew, *Cytochromes c: Evolutionary, Structural, and Physicochemical Aspects*, Springer-Verlag, Berlin, 1990.
20 S. Hu, I. K. Morris, J. P. Singh, K. M. Smith and T. G. Spiro, *J. Am. Chem. Soc.*, 1993, **115**, 12446.
21 T. Uno, Y. Nishimura and M. Tsuboi, *Biochemistry*, 1984, **23**, 6802.
22 D. S. Cohen and G. J. Pielak, *Protein Sci.*, 1994, **3**, 1253.

23 T. Kitagawa, Y. Ozaki, J. Teraoka, Y. Kyogoku and T. Yamanaka, *Biochim. Biophys. Acta*, 1977, **494**, 100.
24 Y. P. Myer, R. B. Srivasatava, S. Kumar and K. Raghvendra, *J. Protein Chem.*, 1983, **2**, 13.
25 B. Cartling, *Biological Applications of Raman Spectroscopy*, ed. T. G. Spiro, Wiley, New York, Vol. III, 1988.
26 C. Bull, R. G. Fisher and B. M. Hoffman, *Biochem. Biophys. Res. Commun.*, 1974, **59**, 140.
27 E. Culotta and D. E. Koshland, *Science*, 1992, **258**, 1862.
28 T. Malinski and Z. Taha, *Nature* (*London*), 1992, **358**, 676.
29 J. Goretski and T. C. Hollocher, *J. Biol. Chem.*, 1988, **263**, 2316.
30 M. P. Doyle and J. W. Hoekstra, *J. Inorg. Biochem.*, 1981, **14**, 351.
31 O. C. Zafiriou and M. McFarland, *Anal. Chem.*, 1980, **52**, 1662.
32 K. Kikuchi, T. Nagano, H. Hayakawa, Y. Hirata and M. Hirobe, *J. Biol. Chem.*, 1993, **268**, 23106.
33 K. Ishii, H. Sheng, T. D. Warner, U. Forstermann and F. Murad, *Am. J. Physiol.*, 1991, **261**, H598.
34 J. W. Aylott, D. S. Richardson and D. A. Russell, *Chem. Mater.*, 1997, **9**, 2261.
35 S. L. R. Barker, R. Kopelman, T. E. Meyer and M. A. Cusanavich, *Anal. Chem.*, 1998, **70**, 971.
36 F. T. Bonner and M. N. Hughes, *Commun Inorg. Chem.*, 1988, **7**, 215.
37 L. J. Ignarro, H. Lippton, J. C. Edwards, W. H. Baricos, A. L. Hyman, P. J. Kadowitz and C. A. Gruetter, *J. Pharmacol. Exp. Ther.*, 1981, **218**, 739.

Paper 8/05541F